0.05) higher levels of III in the plasma than those achieved from tablet dosage forms.

Although such differences have not been observed in humans (25), it is possible that the presence of a cosolvent, such as polyethylene glycol, in the dog gut provided an effective dissolution medium for I, thus allowing increased amounts of the drug to be absorbed over a given period of the drug transit in the GI tract. This could explain the observed differences in the relative bioavailability of I in the plasma from a solution and tablet dosage forms.

REFERENCES

(1) W. H. Barr, *Drug Inform. Bull.*, **3**, 27(1969).

(2) J. G. Wagner, "The Physiological Equivalence of Drug Dosage Forms," Department of National Health and Welfare, Canada, 1969, pp. 40–43.

(3) "Bioavailability of Drugs," B. B. Brodie and W. M. Heller, Eds., S. Karger, Basel, Switzerland, 1972.

(4) "Current Concepts in Pharmaceutical Sciences," J. Swarbrick, Ed., Lea & Febiger, Philadelphia, Pa., 1973, pp. 77–96.

(5) WHO Scientific Group, "Bioavailability of Drugs: Principles and Problems", Tech. Rep. Ser. No. 536, WHO, Geneva, Switzerland, 1974.

(6) J. G. Wagner, *Drug Intell. Clin. Pharm.*, **5**, 115(1971).

(7) W. H. Barr, *Pharmacology*, **8**, 55(1972).

(8) L. F. Prescott and J. Nimmo, *Acta Pharmacol. Toxicol., Suppl.*, **3**, 288(1971).

(9) J. G. Wagner, *Drug Intell. Clin. Pharm.*, **4**, 190(1970).

(10) J. Koch-Weser, *N. Engl. J. Med.*, **291**, 233(1974); *ibid.*, **291**, 503(1974).

(11) S. Shaldon, J. R. McLaren, and S. Sherlock, *Lancet*, **1**, 609(1960).

(12) E. J. Ross, *Br. Med. J.*, **1**, 1508(1961).

(13) C. M. Kagawa and V. A. Drill, *Arch. Int. Pharmacodyn. Ther.*, **136**, 283(1962).

(14) N. Gochman and C. L. Gantt, *J. Pharmacol. Exp. Ther.*, **135**, 312(1962).

(15) W. Lowenthal, *Pharm. Acta Helv.*, **48**, 589(1972).

(16) A. M. Sakr, A. A. Kassem, and A. Farrag, *Chem. Aerosol News*, **44**, 37(1973).

(17) C. M. Kagawa, D. J. Bouska, and M. L. Anderson, *J. Pharm. Sci.*, **53**, 450(1964).

(18) C. M. Kagawa, D. J. Bouska, and M. L. Anderson, *Proc. Soc. Exp. Biol. Med.*, **115**, 837(1964).

(19) A. Karim, R. E. Ranney, and H. I. Maibach, *J. Pharm. Sci.*, **60**, 708(1971).

(20) W. Sadée, M. Dagcioglu, and S. Riegelman, *ibid.*, **61**, 1126(1972).

(21) W. Sadée, S. Riegelman, and S. C. Jones, *ibid.*, **61**, 1129(1972).

(22) *Ibid.*, **61**, 1132(1972).

(23) S. Wold, *Technometrics*, **16**, 1(1974).

(24) A. Rescigno and G. Segré, "Drug and Tracer Kinetics," Blaisdell, Waltham, Mass., 1966.

(25) A. Karim, J. Zagarella, T, C. Hutsell, and A. Chao, *Clin. Pharmacol. Ther.*, **19**, 170(1976).

ACKNOWLEDGMENTS AND ADDRESSES

Received August 4, 1975, from the *Departments of Pharmaceutical Research and Development and Drug Metabolism, Searle Laboratories, Chicago, IL 60680*

Accepted for publication January 26, 1976.

The authors thank Mrs. Beatrice Gerstel and Miss Charlotte Craig for technical assistance and Miss Suzanne Sering for manuscript preparation. Appreciation is also expressed to Dr. H. J. Lambert and Dr. E. Lau for suggestions and encouragement.

[x] To whom inquiries should be directed.

Dissolution Rate Equations in Column-Confined Dissolution

J. T. CARSTENSEN [x] and KAILASH DHUPAR

Abstract □ Equations are derived for the dissolution of a soluble solid in a column into a liquid stream. The equations are substantiated by experiments using oxalic acid dihydrate as a test substance. The dissolution rate constant, k, of oxalic acid dihydrate depends on linear velocity, $\bar{v}$ (centimeters per second), by the following equation: $k = (2.54 \pm 0.76) \times 10^{-4}\ \bar{v}$, where k is measured in centimeters per second.

Keyphrases □ Dissolution—soluble solid in a column into a liquid stream, equations derived □ Column-confined dissolution—soluble solid into a liquid stream, equations derived □ Solids, soluble—dissolution in a column into a liquid stream, equations derived

Numerous recent publications have discussed dissolution testing[1]. Pernarowski (1) cited 100 different published methods. LeHir (2) also described the technology in depth.

Some reported work relates to the use (or potential use) of column apparatuses for dissolution of dosage forms (3–13). The scope of this article is the experimental probing of an actual monodisperse system dissolving in a column at low liquid velocities[2]. Oxalic acid was used because it was tested previously under other conditions (14) and found to be easy to reproduce by controlled recrystallization from water.

EXPERIMENTAL

Oxalic acid[3] was recrystallized as the dihydrate and classified by sieving as described previously (14). The dissolution experiments were performed in a column such as the one shown in Fig. 1. A female ground joint (A_1) was fused[4] onto the top of a 50-ml buret. A male ground joint (A_2) was fused onto a sintered-glass filter in a 1-cm i.d. Pyrex tube. A stopcock (C), Pyrex tubing, and a female joint were fused onto the other end of the sintered-glass filter tube, and the tube was bent beyond C at the angle shown. The female joint fit the outlet

[1] There was no attempt here to make a complete bibliography; only articles directly relevant to the particular arguments in this study are cited. For a bibliography of methodology, the reader is referred to Ref. 1.

[2] Reynolds numbers between 10 and 100.

[3] Mallinckrodt analytical reagent oxalic acid dihydrate, Mallinckrodt Chemical Works, Saint Louis, Mo.

[4] All fusing was done by glass blowing using Pyrex glass and a gas–oxygen flame.

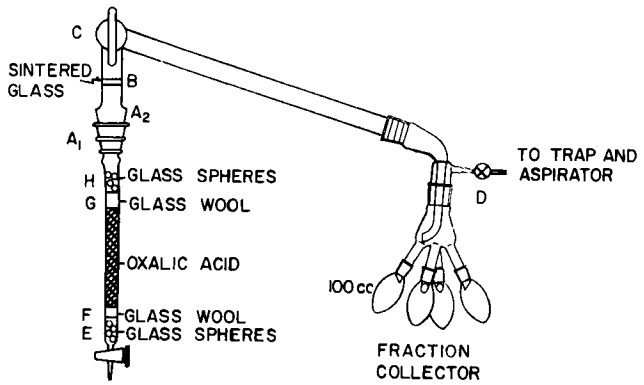

Figure 1—*Apparatus used for dissolution rate studies.*

joint of a commercial glass fraction collector[5] with four 100-ml collecting bulbs.

The vacuum outlet of the fraction collector was connected to an erlenmeyer vacuum flask, serving as a trap; this flask, in turn, was connected to a water aspirator *via* a stopcock (D). The tip of the buret stopcock was attached *via* a piece of Tygon tubing to a micrometric flow valve[6]. The rate of liquid flow could be governed by both this valve and the position of D.

The column was loaded with glass spheres at E to a depth of 1 cm, then with 1 cm of glass wool (at F), and then with 40 cm (~ 33 g) of oxalic acid dihydrate crystals of a given mesh sieve fraction. Glass wool (1 cm) and glass beads (8 cm) were then added at points G and H. The purpose of the glass beads at E is to rectify the turbulence that occurs at the pipe widening beyond the stopcock (5). The purpose of the glass beads at H is to weight down the column so that it does not move upward during experiments performed at high liquid velocity. The purpose of the sintered-glass filter is to prevent passage of entrained small particles into the efflux beyond C.

After the column had been packed, the buret stopcock was closed, C and D were opened, and the aspirator was started. Just prior to the start of the experiment, C was closed, a 500-ml beaker with 0.1 *N* HCl was lifted over the tip of the flow valve, and the buret stopcock and C then were opened. Timers were started, and the time required to fill each of the four collecting bulbs (t_i) was recorded. The collector was turned by hand at the point when collection was changed from one bulb to the next.

The length of the column[7] as a function of time was recorded by noting the time at which the column reached prefixed marks at the buret and then noting the position of the top of the column; the latter

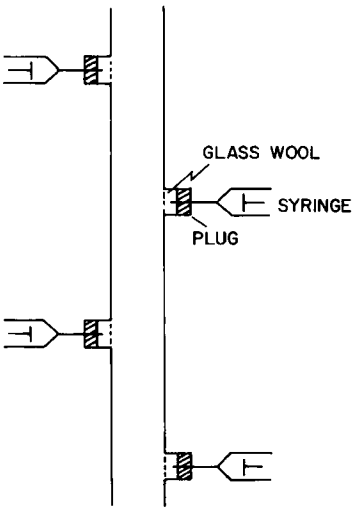

Figure 2—*Apparatus for studying the dependence of* C *on* x.

[5] Catalog No. 10525 and No. 10515, Eck and Krebs Scientific Laboratory Glass Apparatus Inc., Long Island City, NY 11101

[6] Catalog No. M7110, Roger Gilmon Instruments Inc., Great Neck, NY 11021

[7] Two persons are needed to collect results from one experiment.

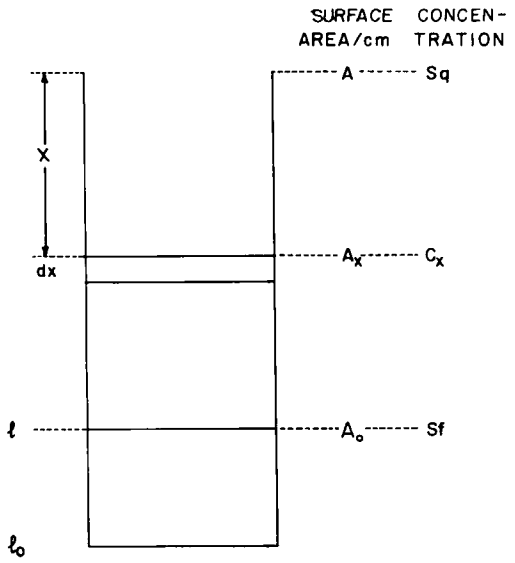

Figure 3—*Nomenclature used.* A_x = *surface area per centimeter of column length,* x = *distance from top of column,* l = *length of column at time* t, S = *saturation concentration,* f = *degree of saturation of feed,* q = *degree of saturation of efflux and* C_x = *concentration at point* x *in the column.*

moved very slightly downward (3 mm during an experiment). The volume flow rate, V (milliliters per second), could then be calculated by weighing the collected fraction (w_i) and dividing by the density (ρ_i) and the time elapsed for the collection (t_i). The densities, ρ_i, were obtained by pycnometry; the amount of oxalic acid present in a fraction (x_i) was determined titrimetrically.

The feeds used in the experiments were (*a*) 0.1 *N* HCl and (*b*) 0.1 *N* HCl containing varying concentrations of oxalic acid—*viz.*, degrees of saturation of 0.2, 0.4, 0.6, and 0.8

The specific surface area of a coarse solid as used here is small and cannot be determined by gas adsorption or by permeametry. The geometric surface areas can be obtained by microscopy, since the crystals can be approximated by parallelepipeds (15) of side L, breadth $\alpha\overline{B}$, and height $\overline{B}$. Then $N = 50$ crystals of a 10–20-mesh cut were weighed, and their dimensions (L and $\alpha\overline{B}$) were determined microscopically. The volume was then (since the sample is fairly monodisperse) $\alpha\overline{L}(\overline{B})^2$. Comparing the theoretical weight, $N\alpha\overline{L}(\overline{B})^2(\rho)$ (where $\rho = 1.66$ g/ml) to the actual weight allows calculation of α; hence, the specific geometric surface area can be found to be $(2\alpha\overline{L})(\overline{B}) + 2[\overline{L}(\overline{B})] + 2[\alpha(\overline{B})^2]$. The same procedure was carried out for all mesh fractions.

The surface area term of interest, as will be discussed later, is A, the surface area present in a 1-cm length of column. It is of interest to see if or how A changes as a function of position and time. For this purpose, a column was packed alternately with glass wool and oxalic acid (10–20 mesh); the column, in this fashion, consisted of seven subcolumns. A dissolution experiment was then carried out for 67 sec and the lengths of the various sections were measured. The geometric surface area was then determined microscopically and divided by the length to give the value of A.

At one point, it was desired to check the concentration profile along the column. For this purpose, a duplicate column was prepared, with four side arms (Fig. 2). The sidearms were short (8 mm) and could accommodate a rubber plug, into which a hypodermic syringe was inserted. Prior to insertion of the plug, the space in front of it was filled with glass wool (Fig. 2). At a particular point in an experiment, the flow was stopped and samples were removed from the four positions and assayed for oxalic acid.

RESULTS AND DISCUSSION

Consider a column of solid powder of length l cm and cross section σ cm^2 (Fig. 3). The surface area (square centimeters) of the amount of powder (b g) in 1-cm length of column is denoted A (square centimeters per centimeter). The liquid enters from the bottom of the column at a flow rate of V_i cm^3/sec. It dissolves solid from the column and exits with a rate of V' cm^3/sec, where V' includes the volume in-

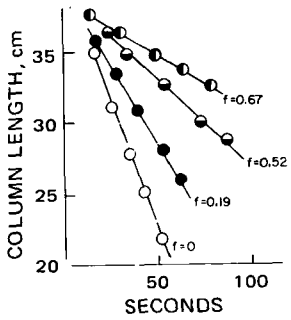

Figure 4—*Column length as a function of time. Key:* ○, f = *0 and* V = *3.42 ml/sec;* ●, f = *0.19 and* V = *2.56 ml/sec;* ⊖, f = *0.52 and* V = *2.53 ml/sec; and* ◐, f = *0.67 and* V = *2.35 ml/sec. Particles are −20/+40 mesh.*

crease due to the dissolved solid. If V denotes the average of V_i and V', then, if ϵ is the porosity of the powder, the magnitude of the average linear velocity (simply denoted the linear velocity, $\bar{v}$) is given by (15):

$$\bar{v} = V/(\sigma\epsilon) \qquad \text{(Eq. 1)}$$

Since σ cm^3 contains b g of density ρ g/ml, the porosity is given by:

$$\epsilon = 1 - (b/\sigma\rho) \qquad \text{(Eq. 2)}$$

It was observed that, under the conditions imposed, the liquid was always fairly close to saturation, S (grams per milliliter), upon exit. If one denotes the exit concentration qS, where q, the degree of saturation, is close to unity, then the following holds: in t sec, Vt ml will have passed through the column and will have saturated to a degree of Sq, *i.e.*, will have dissolved $VtS(q - f)$ g, if the incoming liquid is of a degree of saturation of f. Since there is b g of solid powder per linear column centimeter, $VtS(q - f)/b$ cm will have disappeared, *i.e.*:

$$l = l_0 - \frac{VS(q-f)}{b}t = l_0 - \alpha t \qquad \text{(Eq. 3)}$$

so that the column length should decrease linearly in time. That this is so is seen directly from Fig. 4. The slopes should be proportional to the liquid velocity. That this is so is seen in Fig. 5, where slopes of plots of the type shown in Fig. 4 are plotted against the flow rates, V. The plot is linear and goes through the origin as dictated by:

$$\alpha = [S(q-f)/b]V = \beta V \qquad \text{(Eq. 4)}$$

where:

$$\beta = (S/b)(q-f) = -\frac{S}{b}f + \frac{S}{b}q \qquad \text{(Eq. 5)}$$

Hence, if the slopes, β, from Fig. 5 are plotted *versus* the degree of saturation, f, of the incoming liquid, a linear plot should result; this plot is shown in Fig. 6[8].

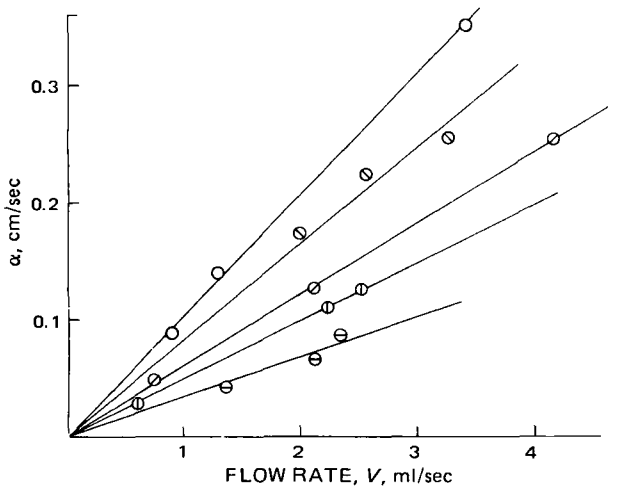

Figure 5—*Column decrease rate, α, as a function of flow rate,* V, *of −20/+40-mesh particles. Key:* ○, f = *0.0;* ⊘, f = *0.19;* ⊘, f = *0.35;* ⊖, f = *0.52; and* ⊖, f = *0.67.*

[8] Here $q \sim 1$ and is considered constant in these plots.

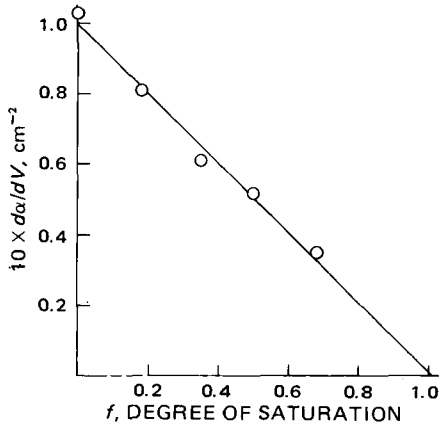

Figure 6—Plot of dα/dV *as a function of* f *for −20/+40-mesh particles.*

It is noted from Fig. 6 that the plot is fairly linear and cuts the f-axis close to $f = q = 1$ in accordance with Eq. 5. The slope in Fig. 6 is − 0.1; *i.e.*, from Eq. 5, S/b should equal 0.1. For the 10–20-mesh cut depicted, there is 36 g of solid/39 cm of column so that b = 36/39. Furthermore, S = 0.13 g/ml so the slope, by these values, should be −0.13/(36/39) = −0.13, *i.e.*, of the same order of magnitude, albeit higher, than the value obtained from the slope in Fig. 6.

When referring to Fig. 3 and using the terminology of this figure, it is noted that a volume element $\sigma\,dx$, which is x cm from the top of the column, contains solid with a surface area of $A_x\,dx$, so that the dissolution rate in this volume element would be:

$$\text{dissolution rate} = kA_x\,dx(S - C_x) \qquad \text{(Eq. 6)}$$

where k (centimeters per second) is the intrinsic dissolution rate constant. Hence, the dissolution rate over the entire column at time t, when the length is l cm, is:

$$dm/dt = \int_0^l kA_x(S - C_x)\,dx \qquad \text{(Eq. 7)}$$

The results from the experimental determination of A_x *versus* x are shown in Fig. 7. It appears[9] (as expected) that A_x is high at the bottom of the solid column and then rapidly drops to a constant value. This drop occurs over a length of less than 3 cm (*i.e.*, less than 10% of the length of the column); therefore, A_x is given by:

$$A_x = A_0 \qquad x < l' \qquad \text{(Eq. 8}a\text{)}$$

$$A_x = A_0 + \zeta(x - l') \qquad l' < x \leq l \qquad \text{(Eq. 8}b\text{)}$$

where ζ is the slope of the nonlinear portion of Fig. 7, and where l' denotes the point where A_x starts increasing (and is close to l, the total

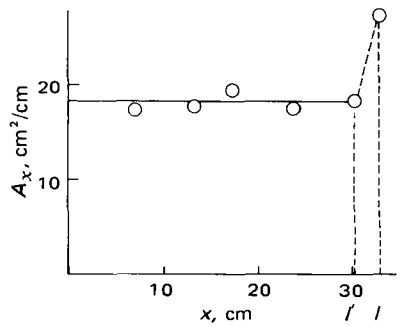

Figure 7—*Surface area per centimeter column length after a dissolution experiment.* A_x *is plotted as a function of* x *for a −10/+20-mesh particle sample.*

[9] For example, the number of particles of diameter d_1 in a single layer (d_1 cm thick) is O/d_1^2, assuming a "square" packing. The solid surface area is then $[O/(d_1^2)]\pi d_1^2 = \pi O$, so that the area per column length is $A_1 = O\pi/(d_1)$. If, after some dissolution, the diameter decreases to d_2, then by a similar argument $A_2 = O\pi/(d_2) > A_1$ (because $d_2 < d_1$).

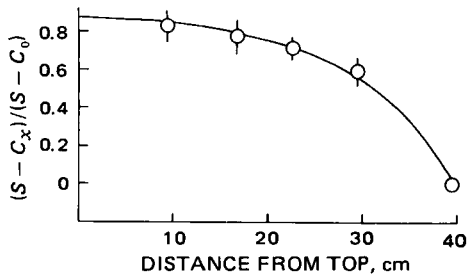

Figure 8—*Concentration,* C_x, *as a function of* x. *Particles are −20/+40 mesh.*

length of the column). Entering this into Eq. 7 then gives:

$$-\frac{dm}{dt} = kA_0 \int_0^l (S - C_x)\,dx + k \int_{l'}^l \zeta(x - l')(S - C_x)\,dx \quad \text{(Eq. 9)}$$

The concentration profile was determined (Fig. 8). The shape of the curve suggests that (with real particles in real packings as opposed to hypothetical spheres with theoretical porosities) the concentration C_x is a function of x by:

$$\ln [(S - C_x)/(S - C_l)] = gx + j \quad \text{(Eq. 10}a\text{)}$$

That this is so is seen in Fig. 9. Since $x = l$ implies that the left-hand side of Eq. 10a is zero, it follows that $0 = gl + j$, *i.e.*, $j = -gl$, so:

$$\ln [(S - C_x)/(S - C_l)] = g(x - l) \quad \text{(Eq. 10}b\text{)}$$

or:

$$S - C_x = (S - C_l)e^{g(x-l)} \quad \text{(Eq. 11)}$$

At $x = 0$, $C_x = Sq$; and since $C_l = Sf$, it follows that:

$$S(1 - q) = S(1 - f)e^{-gl} \quad \text{(Eq. 12}a\text{)}$$

or:

$$e^{gl} = (1 - f)/(1 - q) \quad \text{(Eq. 12}b\text{)}$$

Introducing Eq. 11 into Eq. 9 gives:

$$-\frac{dm}{dt} = kA_0 \int_0^l S(1 - f)e^{g(x-l)}dx + k \int_{l'}^l \zeta(x - l')S(1 - f)e^{g(x-l)}dx \quad \text{(Eq. 13)}$$

It is shown in the *Appendix* that, under the assumption that $l \sim l'$, this equation can be simplified to:

$$-\frac{dm}{dt} = \frac{kA_0Sl(q - f)}{\ln[(1 - f)/(1 - q)]} \quad \text{(Eq. 14)}$$

The rate constants were calculated according to Eq. 14 for all conditions used, and an example of such a calculation is shown in Table I. The experimental values of k obtained in this fashion were then plotted as a function of flow rate (Fig. 10). It is obvious from Table I and from the lengths of the bars in Fig. 10 that the values of k are time independent, *i.e.*, that k indeed is a constant; this finding is experimental support for the views put forth so far.

As mentioned, the time independence of k is implied by the small magnitude of the length of the bars in Fig. 10; these bars are the 95% confidence intervals calculated conventionally (as shown in Table I)

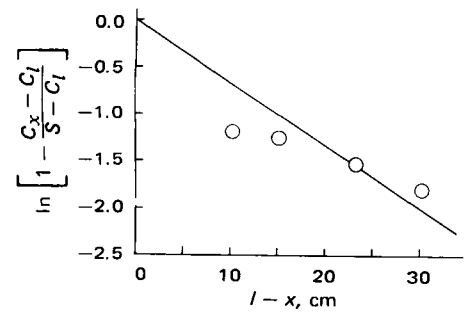

Figure 9—*Data in Fig. 8 plotted as a* σ^- *plot.*

Table I—k Values According to Eq. 14 from a 10–20-Mesh Sample

	V, ml/sec	10^4k, cm/sec
	2.20	43.7
	2.29	41.9
	2.33	42.2
	2.28	45.8
Average	2.27	43.4
$t_{3,0.05}$	3.18	—
σ =	0.054	—
$t\sigma/\sqrt{n} = \gamma$ =	0.086	—

according to $\gamma = t_{0.05}\,\sigma/\sqrt{n}$, where $\sigma\sqrt{n}$ is the standard error and $t_{0.05,n-1}$ is the Student t value for $n - 1$ degrees of freedom.

The least-squares fit line for the data in Fig. 11, weighted by factors of $(1/\gamma)$, is:

$$k = 4.76 \times 10^{-4}\,V - 0.31 \times 10^{-4} \quad \text{(Eq. 15)}$$

where k is in centimeters per second, and V is in milliliters per second.

As discussed later, the liquid velocity is of a magnitude dictating laminar (or slightly turbulent) flow. This flow is presumably the type around a particle in most dissolution methods. Extrapolating to zero velocity is possible *via* Eq. 15, but the confidence limits around this extrapolated value include zero. Carstensen and Patel (14) showed that static dissolution rate constants are at least an order of magnitude smaller than those found from "usual" beaker-type dissolution rate methods.

The flow rates used here (Figs. 5 and 10) are of the order of 2 ml/sec. With a cross section of 0.8 cm^2 and a porosity of 0.4, this rate would give a linear velocity of $2/(0.4 \times 0.8) = 6.25$ cm/sec. For a 20-mesh particle, the diameter is $d = 0.082$ cm, so that the Reynolds number (calculated according to Refs. 16 and 17) is $Re = (vd\rho)/\eta$, where ρ (grams per milliliter) is the density of the liquid and η is the viscosity in poises. Assuming these values to be $\rho = 1.00$ g/ml and $\eta = 0.01$ poise gives $Re = 6.25 \times 0.082 \times 1.0 \div 0.01 \sim 50$. Groves *et al.* (18), in column work with tablets, found backflow at $Re < 10$ and instability at $Re > 100$. Therefore, the flow rates found in the present study correspond to what they found to be a stable range.

The work reported here does *not* intend to describe another dissolution method with application to dosage forms. The apparatus was constructed because it appears to be the best way of creating well-defined linear liquid velocities; the sole intent of its construction was to study the dissolution of an easily reproducible crystal. In the pro-

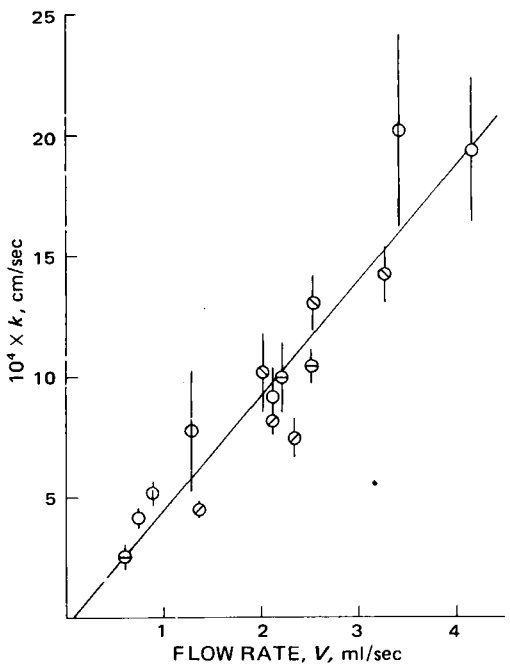

Figure 10—*Dissolution rate constants,* k, *as a function of liquid flow rate,* V.

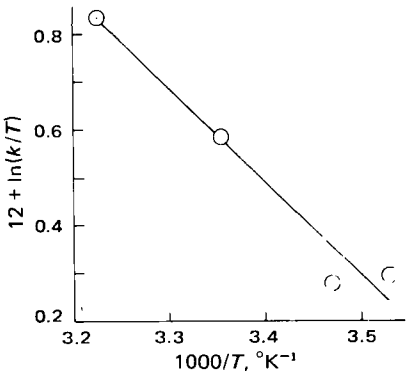

Figure 11—*Plot of* (k/T) *as a function of reciprocal absolute temperature.* E_a = *3900 kcal/mole.*

cess, the equations for dissolution of a dissolving powder in a column-type operation were derived. Mass transport equations for column apparatuses have appeared (19), but they relate primarily to solid supports (which adsorb and desorb solutes from and into the feed but themselves remain of constant weight) and nondisintegrating entities (9). Actual dissolution in columns has been reported (20) but at high Reynolds numbers (100–1000).

Oxalic acid was used because it is easily reproducible in fairly coarse particle size and remains isometric during dissolution (14). The experiments were carried out at a series of temperatures. The k values obtained were plotted as ln (k/T) *versus* $(1/T)$ and, according to Puisieux and Carstensen (21), should be linear with slopes between E_η/R and $2E_\eta/R$, where E_η is the energy of activation of the viscosity of the dissolving liquid. That this is the case is seen in Fig. 11. According to this figure, oxalic acid dihydrate has a dissolution rate constant that can be presented by:

$$\ln (k/T) = -(1880/T) + 6.87 \qquad \text{(Eq. 16)}$$

This gives an activation energy of −3770 cal/mole, which is close to the activation energy of water (−4000 cal/mole).

The least-squares fit shown in Eq. 15 was made with flow rate, V (milliliters per second), as the independent variable. This rate is, in the following, converted to liquid velocity, $\bar{v}$ (centimeters per second), *via* Eq. 1. The intercept value (0.31) is shown not to differ significantly from zero, and the least-squares fits are confined to the zero intercept, *i.e.*, slope = $\Sigma xy/(\Sigma x^2)$. The slopes and 95% confidence limits of the slopes calculated in this fashion are shown in Table II.

It is expected that k values should be a function of $\bar{v}$ and, indeed, at smaller particle sizes they are (21). The studies here failed to show significant differences at the coarse particle sizes tested (Table II). The last line gives the composite value of all mesh fractions tested; *i.e.*, oxalic acid dihydrate has a dissolution rate constant that can be represented by:

$$k = (2.54 \pm 0.76) \times 10^{-4}\,\bar{v} \qquad \text{(Eq. 17)}$$

where k and $\bar{v}$ are in centimeters per second.

SUMMARY

1. Equations for dissolution of a solid in a column into a flowing liquid stream were developed.

2. The results obtained by dissolving oxalic acid dihydrate by such a method are consistent with the equations as far as: (*a*) the column length is a function of time; (*b*) the rate of decrease of the column length is a function of liquid velocity; (*c*) the slope–intercept relations of plots are of type (*b*); (*d*) k, the intrinsic dissolution rate constant, is time independent at a particular velocity; and (*e*) k has the predicted activation energy.

Table II—Slopes of k *versus* $\bar{v}$ Plot

Mesh Fraction	Slope × 10^{-4}	95% Confidence Limits on Slope	Degrees of Freedom
10–20	3.7	1.1	8
20–40	1.8	0.7	14
40–60	1.2	0.6	8
60–80	1.2	0.8	8
Composite	2.54	0.76	41

APPENDIX

Equation 13 may be written:

$$-\frac{e^{gl}}{kS(1-f)}\frac{dm}{dt} = A_0\int_0^l e^{gx}\,dx + \zeta\int_{l'}^{l} xe^{gx}\,dx - \zeta l'\int_{l'}^{l} e^{gx}\,dx \qquad \text{(Eq. A1)}$$

The substitution $u = gx$ (*i.e.*, $dx = (1/g)du$) is then made with the appropriate change in the limits: for $x = 0$, $u = 0$; for $x = l$, $u = gl$. Equation A1 then becomes:

$$-\frac{e^{gl}}{kS(1-f)}\frac{dm}{dt} = \frac{A_0}{g}\int_0^{gl} e^u\,du + \frac{\zeta}{g^2}\int_{gl'}^{gl} ue^u\,du - \frac{\zeta l'}{g}\int_{gl'}^{gl} e^u\,du \qquad \text{(Eq. A2)}$$

Noting that $\int ue^u\,du = ue^u - u$ plus an integration constant allows integration of Eq. A2; multiplying through by g then gives:

$$-\frac{ge^{gl}}{kS(1-f)}\frac{dm}{dt} = A_0(e^{gl}-1) + \frac{\zeta}{g}(gle^{gl} - e^{gl} - gl'e^{gl'} + e^{gl'}) - \zeta l'(e^{gl} - e^{gl'}) \qquad \text{(Eq. A3)}$$

With the assumption that $l \sim l'$ so that also $e^{gl} \sim e^{gl'}$, the last two parentheses vanish and the equation becomes:

$$-\frac{ge^{gl}}{kS(1-f)}\frac{dm}{dt} = A_0(e^{gl}-1) \qquad \text{(Eq. A4)}$$

Introducing Eq. 12 for e^{gl} and the logarithmic form of Eq. 12 for g:

$$g = (1/l)\ln[(1-f)/(1-q)] \qquad \text{(Eq. A5)}$$

into Eq. A4 then gives:

$$-\frac{(1/l)\{\ln[(1-f)/(1-q)]\}[(1-f)/(1-q)]}{kS(1-f)}\frac{dm}{dt} = A_0\left[\frac{(1-f)}{(1-q)} - 1\right] \qquad \text{(Eq. A6)}$$

which is synonymous with Eq. 14.

REFERENCES

(1) M. Pernarowski, in "Dissolution Technology," L. Leeson and J. T. Carstensen, Eds., IPT of APhA Academy of Pharmaceutical Sciences, Washington, D.C., 1974, p. 58.

(2) A. LeHir, "Abrégé de Pharmacie Galénique," Masson et Cie, Paris, France, 1974, p. 109.

(3) J. T. Carstensen, in "Dissolution Technology," L. Leeson and J. T. Carstensen, Eds., IPT of APhA Academy of Pharmaceutical Sciences, Washington, D.C., 1974, p. 19.

(4) R. J. Whithey and A. J. Bowker, *J. Pharm. Pharmacol.*, **24,** 346(1972).

(5) J. Tingstad, J. Dudzinski, L. Lachman, and E. Shami, *J. Pharm. Sci.*, **62,** 1527(1973).

(6) J. E. Tingstad and S. Riegelman, *ibid.*, **59,** 692(1970).

(7) J. E. Tingstad, E. Gropper, L. Lachman, and E. Shami, *ibid.*, **61,** 1985(1972).

(8) *Ibid.*, **62,** 293(1973).

(9) F. Langenbucher, *J. Pharm. Sci.*, **58,** 1265(1969).

(10) K. Marshall and D. B. Drook, *J. Pharm. Pharmacol.*, **21,** 790(1969).

(11) D. C. Baun and G. C. Walker, *J. Pharm. Sci.*, **58,** 611(1969).

(12) C. F. Lerk and K. Zuurman, *J. Pharm. Pharmacol.*, **22,** 319(1970).

(13) A. Richter, R. Myhre, and S. C. Khama, *ibid.*, **21,** 409(1969).

(14) J. T. Carstensen and M. Patel, *J. Pharm. Sci.*, **64,** 1770(1975).

(15) W. A. Gray, "The Packing of Solid Particles," Chapman and Hall, Ltd., London, England, 1968, p. 129.

(16) V. G. Levich, "Physicochemical Hydrodynamics," Prentice-Hall, Englewood Cliffs, N.J., 1962, p. 7.
(17) F. Langenbucher, *Pharm. Acta Helv.*, **49**, 187(1974).
(18) M. J. Groves, M. H. Alkan, and M. A. Deer, *J. Pharm. Pharmacol.*, **27**, 400(1975).
(19) S. Ergun, *Chem. Eng. Progr.*, **48**, 227(1952).
(20) J. W. Mullen and T. P. Cook, *J. Appl. Chem.*, **15**, 145(1965).
(21) F. Puisieux and J. T. Carstensen, *Ann. Pharm. Fr.*, in press.

ACKNOWLEDGMENTS AND ADDRESSES

Received August 4, 1975, from the *School of Pharmacy, University of Wisconsin, Madison, WI 53706*
Accepted for publication January 21, 1976.
[x] To whom inquiries should be directed.

Microenvironmental Kinetic Effects within a Lyotropic Smectic Biophase Model: Conformational Restrictions in Fischer Indole Cyclization

HUSSEIN G. IBRAHIM [*] and EDWARD G. RIPPIE [x]

Abstract □ The microenvironmental orientation effects, arising from an ordered solvent structure, were studied in a model liquid crystalline biophase for the cyclization of a series of 2-substituted cyclohexanone phenylhydrazones. The magnitude of such solvent-induced intramolecular conformational constraints was determined from a comparison of the kinetics of the Fischer indole rearrangement in a lyotropic smectic liquid crystal *versus* those in an isotropic liquid of similar chemical composition but lacking the structured nature of the mesophase. Solutions consisting of 50% (w/w) polyoxyethylene 6 tridecyl ether or 44% (w/v) polyethylene glycol in aqueous buffers comprised the smectic or isotropic media, respectively. The apparent dissociation constants of the conjugate acids of the phenylhydrazones were determined kinetically, as were their partition coefficients between lipid and polar isotropic phases approximating the compositions of the smectic lamellae. Intrinsic first-order rate constants, corrected for partitioning within the lamellar mesophase, were used to compute the enthalpies and entropies of activation. The somewhat slower intrinsic rates of cyclization and the accompanying less negative entropies of activation generally observed in the liquid crystalline medium, as opposed to the isotropic system, are attributed to the orienting effects of the lamellar lyotropic mesophase.

Keyphrases □ Cyclohexanone phenylhydrazones, 2-substituted—cyclization reaction kinetics, effect of ordered solvent structure on microenvironmental orientation and intramolecular conformational constraints □ Phenylhydrazones, 2-substituted cyclohexanone—cyclization reaction kinetics, effect of ordered solvent structure on microenvironmental orientation and intramolecular conformational constraints □ Cyclization reaction kinetics—2-substituted cyclohexanone phenylhydrazones, effect of ordered solvent structure □ Solvent structure, ordered—effect on cyclization reaction kinetics of 2-substituted cyclohexanone phenylhydrazones □ Conformational constraints, intramolecular—2-substituted cyclohexanone phenylhydrazones, effect of ordered solvent structure □ Orientation, microenvironmental—2-substituted cyclohexanone phenylhydrazones, effect of ordered solvent structure

Mobile liquid crystalline phases composed of nonrandomly oriented molecules constitute the media for many, if not most, catalytic processes at the cellular level (1–3). In such cases, it is likely that they modify the rates and extent of biochemical reactions and receptor site interactions as well as the processes of active and passive transport. Investigation of the influences of such structured environments on the kinetics and thermodynamics of chemical reactions may explain the nature of their control of the biological processes occurring within them.

BACKGROUND

It is extremely difficult to assess the functions and effects of ordered fluids in a biological system by direct experimentation on living matter. Results from kinetic and thermodynamic solution studies in structured lyotropic solvents, such as the liquid crystals used in this work, can reveal significant information concerning both intra- and intermolecular orientation effects arising solely from the medium structure. Effects of solvent-hindered molecular mobility and the influence of various liquid crystalline structural features on reaction rates also indicate the relative importance of molecular grouping and interaction factors in mesophasic solvent systems and provide a basis for an understanding of the effects of the structured environment on the behavior of drugs in living organisms.

The principal structural feature characteristic of the liquid crystalline state is the parallel arrangement of the component molecules, with rotation primarily being permitted only about the long axis. Because of increasing interest in the mesomorphic states, the characteristic features and properties associated with these systems have been extensively reviewed (4, 5). However, studies of reaction kinetics in such novel solvents are relatively few (6–10).

Since solute species (reactants) dissolved in liquid crystalline media lose freedom of molecular motion to varying degrees due to microenvironmental effects arising from solvent structure, orientation-dependent rearrangement or cyclization reactions can be expected to undergo substantial entropic changes. Also, because of the specific orientations that reactant molecules experience in such ordered fluids, solvent-induced changes in conformation populations can influence significantly any stereospecificity characteristic of the reaction.

Preliminary studies of certain polymerization processes indicated that the molecular order of a nematic solvent often directs the reaction, generally forming isotactic polymers in preference to atactic ones (6). It is also known that molecular diffusion fluxes are functions of molecular orientation as well as the usual driving forces of diffusion. Thus, a reactant molecule dissolved in an ordered fluid experiences anisotropic or directed diffusion, which can significantly affect the kinetics of certain diffusion-controlled reactions.

Fendler and Fendler (11) stressed the importance of studies of chemical reactions in micellar systems because of the recognized analogies between micellar and solvated protein structures and between micellar and enzymatic catalysis. Most of these studies have been conducted in dilute micellar solutions. However, since lyotropic liquid crystals can be regarded as bulk micellar media, they probably would be more representative and better suited for such an analogy.